

Received 14 October 2019; reviewed; accepted 15 January 2020

Effects of copper ions on malachite sulfidization flotation

Wanzhong Yin ^{1,2}, Qiuyue Sheng ¹, Yingqiang Ma ^{3,4}, Haoran Sun ¹, Bin Yang ¹, Yuan Tang ¹

¹School of Resources & Civil Engineering, Northeastern University, Shenyang 110819, China

²Northeastern University Genetic Mineral Processing Research Center, Shenyang 110819, China

³School of Zijin Mining, Fuzhou University, Fuzhou, Fujian 350108, China

⁴State Key Laboratory of Mineral Processing, Beijing 102628, China

Corresponding authors: sqy13110636550@163.com (Qiuyue Sheng), mayingqiang@mail.fzu.edu.cn (Yingqiang Ma)

Abstract: In this study, the effects of copper ions (Cu^{2+}) on the sulfidization (Na_2S) flotation of malachite was investigated using micro-flotation experiments, zeta-potential measurements, X-ray photoelectron spectroscopy (XPS) analysis, adsorption experiments, and Materials Studio simulation. The results indicated that the flotation recovery of malachite decreased after the pretreatment of the mineral particles with Cu^{2+} ions prior to the addition of Na_2S . The results for zeta-potential measurements and XPS analysis revealed that less sulfide ion species in the pulp solution transferred onto the mineral surface, the sulfidization of malachite surface weakened. The adsorption amount of collector on the mineral surface decreased, and this finding was confirmed by the results of the zeta-potential and adsorption experiments. Materials Studio simulation revealed that the adsorption energy of HS^- ions and $\text{C}_4\text{H}_9\text{OCCS}^-$ ions on malachite surface increased after the adding of Cu^{2+} ion. The competitive adsorption made Cu^{2+} ions depress sulfidization flotation of malachite, the dissolution of mineral surface affected the adsorption of reagents on it, and decreased the floatability of malachite.

Keywords: malachite, sulfidization flotation, Cu^{2+} ions, depression

1. Introduction

Copper oxide minerals, mainly including malachite cuprite and azurite, are indispensable copper resource reserves that have gained widespread attention in the fields of beneficiation and metallurgy (Corin et al., 2017; Feng et al., 2017). Due to the higher solubility and extensive hydration, sulfidization flotation is widely used to enrich copper oxide minerals (Liu et al., 2016).

Sulfidization is the critical stage for the malachite sulfidization flotation, HS^- is the substantial reactant that interacts with the malachite surface (Sun et al., 2012; Feng et al., 2015; Shen et al., 2019). The sulfidization product is formed on malachite surfaces including cuprous monosulfide, cuprous disulfide, and cuprous polysulfide, the disulfide and polysulfide determines the sulfidization flotation performance of malachite (Feng et al., 2017), which facilitates the absorption of xanthate collector. The interaction between HS^- and malachite surfaces may involve ion exchange and redox reactions (Park et al., 2016). Copper of the minerals surface plays a key role in the malachite sulfidation flotation (Srdjan 2010). The surface properties of malachite are complex and soluble, the ions dissolved from minerals may affect their sulfidization flotation.

The surface properties and flotation performance of the malachite has gained increasing research attention. The interaction mechanism between the Na_2S and malachite surfaces has been investigated through solution measurements, surface analysis, and density functional theory calculation (Feng et al., 2017). Different types of activators such as ethanediamine and combination of ammonium-amine salt, are used to improve the flotation performance of malachite (Feng et al., 2018). Due to the dissolution, Cu^{2+} ion flood in the flotation pulp, competitive adsorption for flotation reagent between Cu^{2+} ion in

pulp and mineral surface may produce. The solubility of malachite was studied by calculation of the solution chemistry (Hope et al., 2010), but its influence on malachite flotation requires further study.

This study was aimed to investigate the effect of Cu^{2+} ions on the sulfidization flotation behavior of malachite. Flotation experiments, zeta potential measurements, adsorption studies, X-ray photoelectron spectroscopy (XPS) analysis, and density functional theory calculation were carried out to investigate the interaction between sulfide species, collector, and malachite surfaces in the absence and presence of Cu^{2+} ions.

2. Materials and methods

2.1. Materials

The malachite sample used in all experiments was obtained from Kolwezi mine. The sample was first crushed and hand-sorted, the crushed sample was ground and sieved to obtain particles size of $-106+45\ \mu\text{m}$ for the micro-flotation, XPS analysis, and adsorption measurements. X-ray diffraction (XRD) result of the sample seen in Fig. 1 and chemical analysis presented in Table 1 indicated the sample with 52.18% Cu, the theoretical content of Cu in malachite ($\text{CuCO}_3\text{Cu}(\text{OH})_2$) was 57.57%, which revealed that the malachite content in sample was 90.50%. Na_2S (Baiyin Nonferrous Metals Co. Ltd., AR grade) and sodium butyl xanthate (NaBX, Hunan Mingzhu mineral processing agent Co.Ltd., GR grade) were employed as a sulfidizing agent and a collector, respectively. Hydrochloric acid (HCl, Xilong Chemical Co.Ltd., AR grade) and sodium hydroxide (NaOH, Xilong Chemical Co.Ltd., AR grade) were used to regulate solution pH. CuSO_4 (Xilong Chemical Co.Ltd., AR grade) was used to study the effects of copper ions on malachite sulfidization flotation. Deionized water (DI, Resistivity = 18.25 $\text{M}\Omega\cdot\text{cm}$, Shenyang Xinjie Technology Co., Ltd, XJG-20-A) was used for all of the experiments.

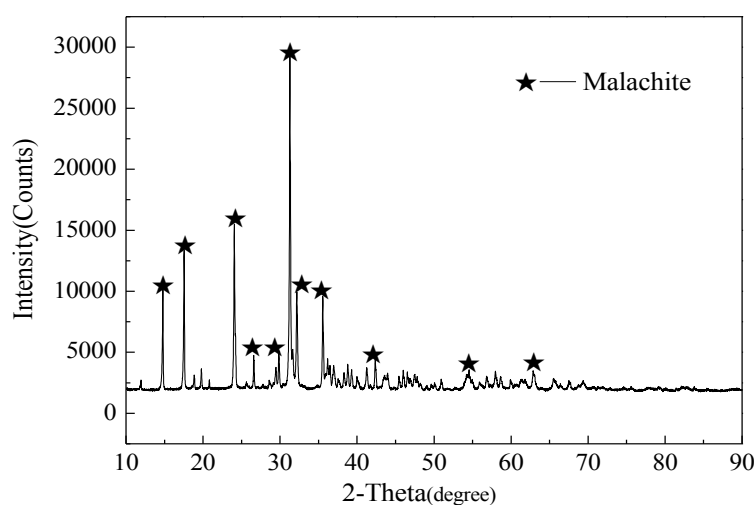


Fig. 1. XRD analysis of the sample

Table 1. Chemical analysis of the sample

Cu (%)	SiO_2 (%)	C (%)	P_2O_5 (%)	Purity (%)
52.18	5.98	4.78	1.82	90.50

2.2. Methods

2.2.1. Flotation experiments

The flotation of a single mineral was carried out using an XFGCII laboratory flotation cell (Jilin Exploration Machinery Plant, China) with a volume capacity of 40 cm^3 at a spindle speed of 1992 rpm. For each flotation test, 2 g of malachite sample was first placed into the flotation cell. HCl and NaOH solutions were used to adjust the pH, and the reagents were added to the cell if needed in the following

order: CuSO_4 , Na_2S , NaBX , 2#oil, conditioned for 3 min with each reagent, then, followed by 3 min flotation collection. Finally, the froth stream was weighed after drying to obtain the flotation recovery of malachite, each flotation test was conducted at least three times, and the average results were calculated with a typical variation of $\pm 1.8\%$.

2.2.2. Zeta-potential measurements

The zeta-potential measurements of malachite were conducted using a Nano-ZS90 zeta-potential analyzer (Malvern Instruments Ltd., Britain). The malachite sample was finely ground to $-5\ \mu\text{m}$ in an agate mortar, and *DI* water was added to obtain the 0.01% solids ratio of the suspension solution. Then, the desired reagents and $3 \times 10^{-4}\ \text{mol/dm}^3$ of KNO_3 as an electrolyte background were added into the suspension. HCl and NaOH were used to adjust the pH values of the solution. After stirring the suspension for 3 min, the suspension was kept for 3 min to allow the coarse particles to settle down. The supernatant of the suspension was transferred to the measurement vessel for the zeta potential measurements, and the zeta potential was measured as a function of pH. Each value was the average of three measurements with a typical variation of $\pm 2\ \text{mV}$.

2.2.3. X-ray Photoelectron Spectroscopy (XPS) analysis

XPS analysis was performed by an America Thermo VG ESCALAB 250Xi spectrometer using $\text{Al } \alpha$ X-rays (1486.6 eV) as a sputtering source at a power of 150 W (15 kV 10 mA). The binding energy scale was corrected based on a C1s peak from contaminations (around 284.8 eV) as the internal binding energy standard. In the XPS tests, 2 g of malachite sample was conditioned by the same conditioning process used for the micro-flotation experiments, the solid particles were collected, and dried at room temperature for the XPS analysis. The relative contents of elements on malachite surfaces under different conditions were determined, and a precise scan was performed to obtain the XPS spectrum of the specific elements.

2.2.4. Adsorption measurements

The UV-2100 Spectrophotometer was used to measure the adsorption of NaBX on the malachite surface under different conditions. Full-wave scanning showed that the main absorption peak of NaBX occurred at 301 nm, which was used to determine the collector concentration. A series of NaBX aqueous solutions of known concentrations were characterized and recorded in order to correlate their absorbance intensities with their concentrations. The solutions after adsorption were characterized, and the concentrations of NaBX were obtained by comparing their absorbance intensities with those of solutions of known concentration. In the adsorption tests, 2 g of malachite sample was conditioned by the same conditioning process used for the micro-flotation experiments. The amount of collector adsorbed on the mineral surface was calculated by subtracting the residual concentration in the solution from the initial concentration as shown in Eq. (1):

$$\Gamma = \frac{(C_0 - C_r)v}{1000w} \quad (1)$$

where C_0 is an initial concentration (mg/dm^3), C_r is a residual concentration (mg/dm^3), Γ is a adsorption quantity (mg/g), w is the weight of mineral sample (g), v is the volume of solution (cm^3).

2.2.5. Materials Studio calculation

Adsorption is a process in which the molecular motion speed slowed down and eventually stops on the surface of the adsorption medium. When the speed decreases, some energy will be released, which is the adsorption energy. A model of malachite was constructed based on the crystal data, and a further geometry optimization was performed. The surfaces were obtained from the optimized bulk structure. The adsorption studies were performed using the optimized malachite surface. All calculations were done using the CASTEP, GGA-PBESOL in Materials Studio 8.0, the following parameters were fixed during the optimization and simulation process: (a) Energy, (b) Max. force, (c) Max. stress, (d) Max. displacement of $2.0 \times 10^{-5}\ \text{eV/atom}$, $0.05\ \text{eV/\AA}$, $0.1\ \text{GPa}$, $0.002\ \text{\AA}$, respectively. Based on the test results,

the plane wave cut-off energy of 571.4 eV was used for all calculations. The adsorption energy of flotation reagents on the malachite surface was calculated according to Eq. (2):

$$\Delta E = E_a - E_s - E_c \quad (\text{Li et al., 2012}) \quad (2)$$

where ΔE represents the adsorption energy, E_a represents the total energy of the malachite surface with reagents adsorbed, E_s represents the total energy of the malachite surface, and E_c represents the total energy of reagents before adsorption onto the mineral surface. A more negative value of ΔE indicated stronger adsorption of reagents on mineral surface.

3. Results and discussion

3.1. Flotation experiments

The flotation recoveries of malachite as a function of Na_2S and NaBX concentration, and pH are shown in Figs. 2, 3, and 4, respectively.

The flotation recovery of malachite at 80 mg/dm³ of NaBX as a function of Na_2S concentration is shown in Fig. 2. When Na_2S was added prior to NaBX, the flotation recovery of malachite sharply increased from 17.30% to 78.20% by the addition of 80 mg/dm³ Na_2S . Then, the flotation recovery dropped down with further increasing Na_2S . An appropriate amount of Na_2S facilitated malachite floatability, and the malachite was depressed during sulphidization flotation when excess Na_2S was added, as reported in the previous study (Castro et al., 1974; Feng et al., 2017; Shen et al., 2019).

The flotation recovery of malachite at 80 mg/dm³ of Na_2S as a function of NaBX concentration is shown in Fig. 3. It was found that when the concentration of NaBX was 80 mg/dm³, the maximum recovery reached.

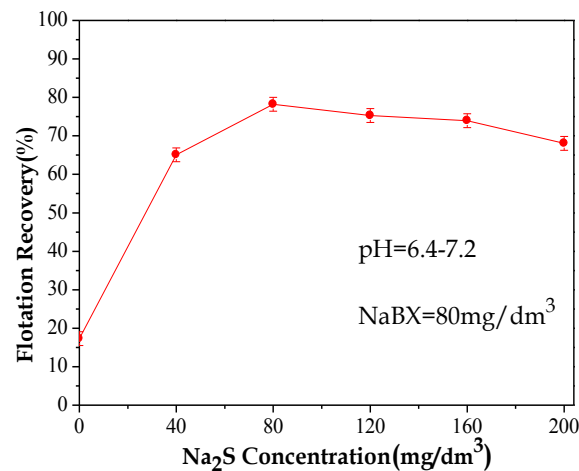


Fig. 2. Effect of Na_2S concentration on malachite flotation

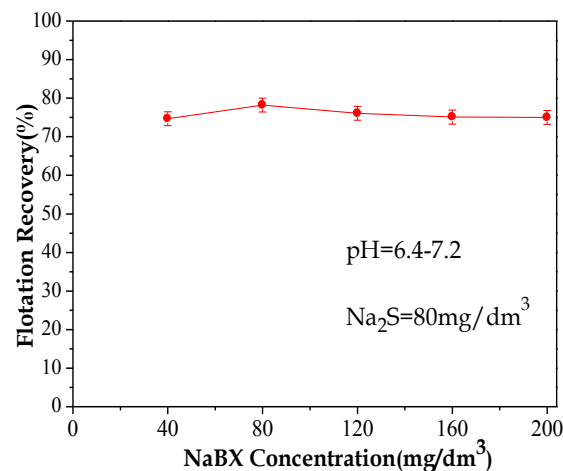


Fig. 3. Effect of NaBX concentration on malachite flotation

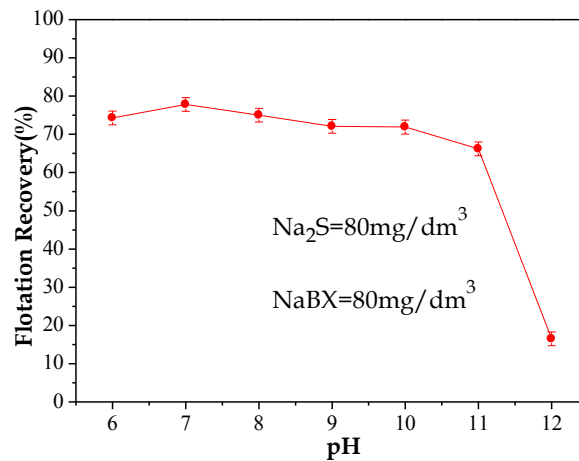


Fig. 4. Effect of pH values on malachite flotation

The flotation of malachite as a function of pH values at 80 mg/dm³ of NaBX and 80 mg/dm³ of Na₂S is presented in Fig. 4. Malachite recovery increased from pH 6-7, and then decreased steadily until at pH=11. Then, the flotation recovery dropped down to a low value with further increasing pH to 12, which was similar to the results in the literature (Liu et al., 2018; Yin et al., 2019).

The flotation of malachite as a function of Cu²⁺ concentration at 80 mg/dm³ of Na₂S, 80 mg/dm³ of NaBX is shown in Fig. 5(a), Cu²⁺ were added in the form of CuSO₄. When CuSO₄ was added prior to Na₂S, the flotation recovery of malachite sharply decreased from 78.20% to 26.90% by the addition of 150 mg/dm³ CuSO₄. This indicated that the addition of CuSO₄ depressed the malachite sulfidization flotation.

The flotation of malachite as a function of pH using 80 mg/dm³ of Na₂S, 80 mg/dm³ of NaBX in the absence and presence of 150 mg/dm³ CuSO₄ is shown in Fig. 5(b). The flotation recovery of malachite decreased after the addition of CuSO₄ over the whole tests pH range. When the pH 6-8, CuSO₄ had a stronger inhibition for the sulfidization flotation of malachite.

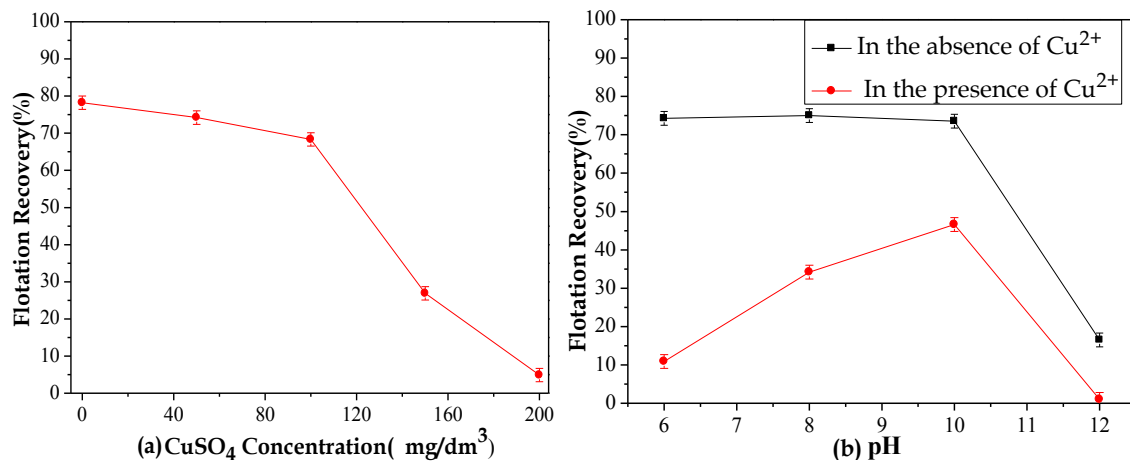


Fig. 5. Effect of Cu²⁺ on malachite flotation

3.2. Depression mechanism of copper ions on malachite sulfidization flotation

3.2.1. Solution chemistry of copper ions

By solution chemical calculation (Powell et al., 2007), the concentrations of each copper species as a function of pH at a total copper concentration of 150 mg/dm³ is shown in Fig. 6. A similar calculation involving Cu species distribution has been studied and reported in previous studies (Feng et al., 2018; Huang et al., 2019). At pH below 7, Cu²⁺ was the predominant species. At pH above 7, Cu(OH)₂(s) produced and became predominant species. Cu(OH)₂(s) may adhere to the surface of malachite, and decrease adsorption quantity of flotation reagents. When the pH 6-8, the Cu²⁺ accounted for a large

proportion, the results of the flotation tests showed that at the pH 6-8, CuSO_4 had a stronger inhibition for the malachite sulfidization flotation, Cu^{2+} in the pulp may form competitive adsorption with copper ions on the malachite surface for reagents, and depress the sulfidization flotation of malachite.

3.2.2. Zeta-potential measurements

The adsorption of sulfide ion and xanthate species onto the malachite surface may influence the zeta potential of the malachite particles. The zeta potential measurements were performed to estimate the interaction between malachite particles and reagents in the flotation experiments, and study the influence of Cu^{2+} for the adsorption of sulfide ion and xanthate species onto the malachite surface. Figure 7 shows the zeta potentials of malachite particles under different conditions as a function of pH. As shown in Fig. 7, the zeta potential of malachite became more negative with the increasing pH values regardless of the addition of flotation reagents.

The isoelectric point (*IEP*) of malachite without the addition of flotation reagents was located at approximately pH 8.6, which was near to the value in previous study (Li et al., 2015; Choi et al., 2016; Liu et al., 2016; Wu et al., 2017; Feng et al., 2018; Liu et al., 2018; Huang et al., 2018; Yin et al., 2019). After the addition of Na_2S , the zeta potential of malachite was more negative than that of bare malachite, sulfide ion species with negative charges were adsorbed onto the malachite surface (Park et al., 2016; Feng et al., 2018; Yin et al., 2019). At the same concentration of Na_2S , the addition of Cu^{2+} made the zeta potential of malachite more positive, this result indicated that less amounts of sulfide ion species were adsorbed onto the malachite surface in the presence of Cu^{2+} than in the absence of it. The Cu^{2+} in pulp

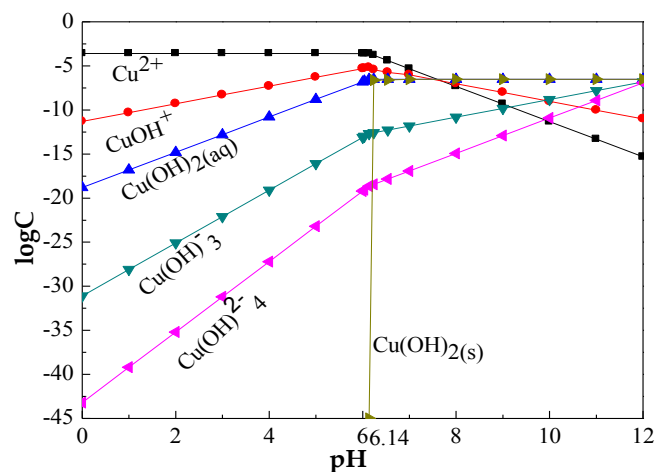


Fig. 6. Calculations of the concentration of each copper species as a function of pH at a total copper concentration of 150 mg/dm^3

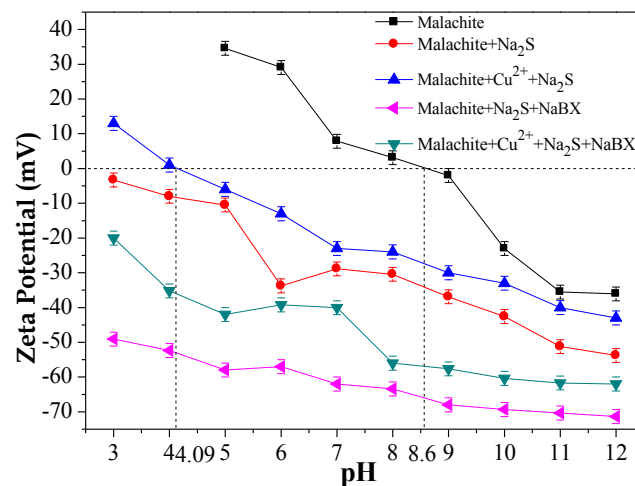


Fig. 7. Zeta potential of malachite as a function of pH under different conditions

weakened the sulfuration of malachite surfaces, which was not beneficial to the sulfuration flotation of malachite. After the mineral surface was treated with Na_2S and NaBX in the absence and presence of Cu^{2+} , the zeta potential became more negative, and this attributed to the adsorption of sulfide ion and xanthate species onto the malachite surface (Wu et al., 2017; Feng et al., 2018; Yin et al., 2019). The addition of Cu^{2+} led to the increase of the zeta potentials of malachite at the same concentration of Na_2S and NaBX , this may indicate that the decrease of adsorption amount of the Na_2S and NaBX on the malachite surface, and the flotation of malachite was depressed.

3.2.3. Elemental compositions and chemical states on malachite surfaces

The relative contents of C, O, Cu, and S elements on the malachite surface under different conditions, are presented in Table 2. Similar to the previous literature (Feng et al., 2017), the relative contents of S and Cu elements on the mineral surface increased after malachite was modified with Na_2S , facilitating the attachment of collectors, according to the study (Feng et al., 2017), the simultaneous reduction in the relative contents of C and O elements on the modified mineral surface further demonstrated that the hydrophobicity of malachite surface increased, and improving the floatability of malachite minerals. When CuSO_4 was added prior to Na_2S , the relative contents of S on the malachite surface decreased to 4.06%, thus, the addition of CuSO_4 before Na_2S could depress the formation of copper sulfide species on the malachite surface, the sulfidization of malachite surface weakened, which decreased the adsorption of collectors, this indicated that the addition of CuSO_4 depressed the malachite sulfidization flotation.

Table 2. Relative contents of elements on malachite surfaces under different conditions

	Samples	Elements	Atomic concentrations (%)
1	pH = 8 $\text{Na}_2\text{S} = 0 \text{ mg/dm}^3$ $\text{NaBX} = 80 \text{ mg/dm}^3$	C	30.53
		O	45.70
		Cu	22.78
		S	1.00
2	pH = 8 $\text{Na}_2\text{S} = 80 \text{ mg/dm}^3$ $\text{NaBX} = 80 \text{ mg/dm}^3$	C	28.38
		O	37.91
		Cu	24.31
		S	9.40
3	pH = 8 $\text{Na}_2\text{S} = 80 \text{ mg/dm}^3$ $\text{NaBX} = 80 \text{ mg/dm}^3$ $\text{Cu}^{2+} = 150 \text{ mg/dm}^3$	C	26.56
		O	40.00
		Cu	29.38
		S	4.06

The $\text{S}2\text{p}$ spectra of malachite samples under different conditions are given in Fig. 8. According to previous study (Harvey et al., 1984; Boulton et al., 2003; Khmeleva et al., 2005), the malachite samples sulfidized with Na_2S , the S peaks located at the binding energy values around of 163 eV were attributed to the $\text{S}^{2-n}(n \geq 2)$ species, the binding energy values around of 161 eV were attributed to the S^{2-} species. The presence of S^{2-n} indicated that a slight oxidation occurred in the sulfidization product of malachite and HS^- species in the pulp solution, the oxidation of sulfide is advantageous to the hydrophobicity of minerals (Boulton et al., 2003; Chen et al., 2014; Feng et al., 2017), improving the floatability of malachite. The addition of Cu^{2+} prior to Na_2S weakened the peak of S^{2-n} and S^{2-} , the area inside the curve of $\text{S}^{2-n}(n \geq 2)$ species in the presence of Cu^{2+} was obviously declined. Combining the data in Table 2, at the same Na_2S concentration, the sulfidization products in the presence of Cu^{2+} decreased. This result further confirmed that the Cu^{2+} in pulp weakened the sulfidization of malachite surface, thereby decreasing the malachite floatability. These results were consistent with the results of the flotation experiments.

Figure 9 shows the $\text{Cu}2\text{p}$ XPS spectra of malachite samples under different conditions. The binding energies shift of Cu indicated the differences in the electronic environment among different conditions. Both Cu(II) (cupric) and Cu(I) (cuprous) species were observed based on their distinct binding energies around of 934 eV and 931.5 eV for $\text{Cu}2\text{p}_{3/2}$ (Li et al., 2015; Liu et al., 2016; Lotter et al., 2016). As shown

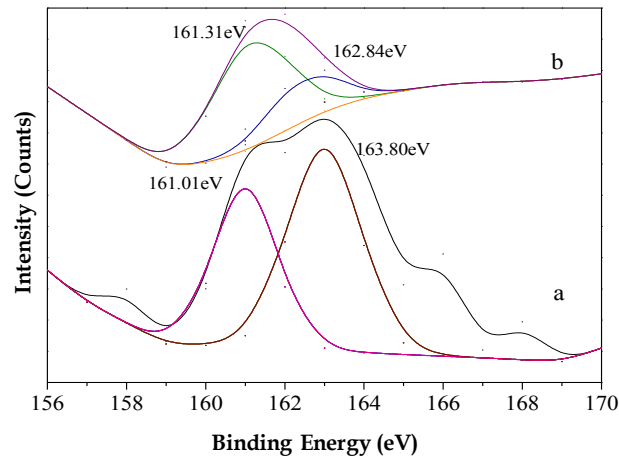


Fig. 8. S2p spectra of malachite samples treated with the following: a: Malachite+Na₂S+NaBX, b: Malachite+Cu²⁺+Na₂S+NaBX

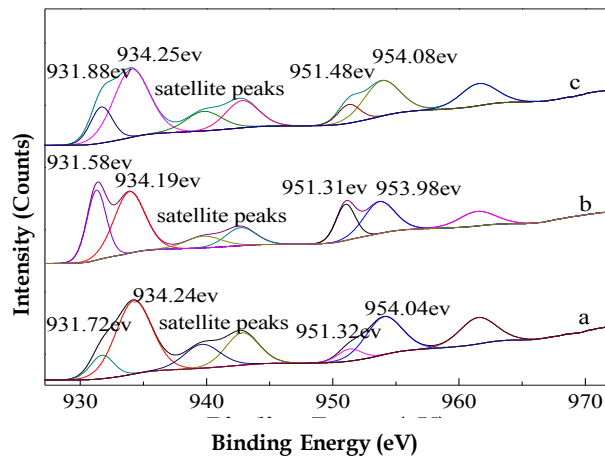


Fig. 9. Cu2p XPS spectra of malachite samples treated with the following: a: Malachite+NaBX, b: Malachite+Na₂S+NaBX, c: Malachite+Cu²⁺+Na₂S+NaBX

in Fig. 9(a) and (b), the area inside the curve of Cu(I) species in the presence of Na₂S was obviously larger than that in the absence of Na₂S, which was consistent with the Feng's work (Feng et al., 2017; Feng et al., 2018). This observation implied that the polysulfide of Cu(I) formed on the mineral surface. In addition, relative amounts of Cu(II) species were reduced to Cu(I) species after malachite was treated with Na₂S, and the area inside the satellite peak decreased because the contents of Cu(II) species in malachite samples were related to satellite peaks (Feng et al., 2017; Feng et al., 2018). The formation of copper sulfide layer was beneficial for the attachment of xanthate species, facilitating the flotation of malachite. As shown in Fig. 9(b) and (c), the area inside the curve of Cu(I) species in the presence of Cu²⁺ was obviously smaller than that in the absence of Cu²⁺. This observation indicated that the addition of Cu²⁺ decreased the amounts of copper sulfide species formed on the malachite surface at the same Na₂S concentration. Which was detrimental for the attachment of xanthate species on malachite surfaces. This result provided evidence for the depression of Cu²⁺ to the sulfidization flotation of malachite. These results were consistent with the results of the flotation experiments.

3.2.4. Adsorption amounts of NaBX onto malachite surfaces

The XPS analysis demonstrated that sulfide ion species in the pulp suspension were transferred onto the mineral surface, the effect was weakened in the presence of Cu²⁺, and less collector may be adsorbed on the malachite surface, to directly illustrate the effect of Cu²⁺ on the collector adsorption on malachite surface, adsorption tests of NaBX onto malachite surfaces was employed in this study. As shown in

Table 3, the addition of Cu^{2+} prior to Na_2S decreased the adsorption amounts of NaBX onto malachite surfaces, depressed the sulfuration flotation of malachite, which was consistent with the XPS analysis.

Table 3. Adsorbed amounts of NaBX onto the malachite surfaces in the absence and presence of Cu^{2+} (80 mg/dm³ of Na_2S , 80 mg/dm³ of NaBX, pH = 8.0)

Samples	Recovery (%)	Residual NaBX concentration C_r (mg/dm ³)	Initial NaBX concentration C_o (mg/dm ³)	NaBX adsorption quantity
In the absence of Cu^{2+} ions	75.00	18.525	80	1.537
In the presence of Cu^{2+} ions	34.20	51.520	80	0.712

3.2.5. Adsorption of $\text{C}_4\text{H}_9\text{OCSS}^-$ and HS^- on the malachite surface

A model of malachite was constructed based on the crystal data received from the American mineralogist crystal structure database, and the cell parameters of malachite are $a=0.9502$ nm, $b=1.1974$ nm, $c=0.3240$ nm, $\beta=98^\circ45'$, the space group is P21/A. According to the previous study (Susse 1966; Zhou 2007; Mao 2016), the optimized malachite crystal structure is shown in Fig. 10. The Mulliken population and the length of the bond in malachite are presented in Table 4. As shown in Table 4, the length order of the bond was $\text{Cu-O} > \text{C-O} > \text{H-O}$, the Mulliken population of the Cu-O smaller than C-O and H-O, the covalent bond strength order in malachite was $\text{C-O} > \text{H-O} > \text{Cu-O}$, which were consistent with the Wu's and Mao's work (Mao 2016; Wu et al., 2017), Cu and O in malachite have higher reactivity (Mulliken, 2004). The flotation reagents mainly react with Cu on the malachite surface (Mao 2016; Wu et al., 2017).

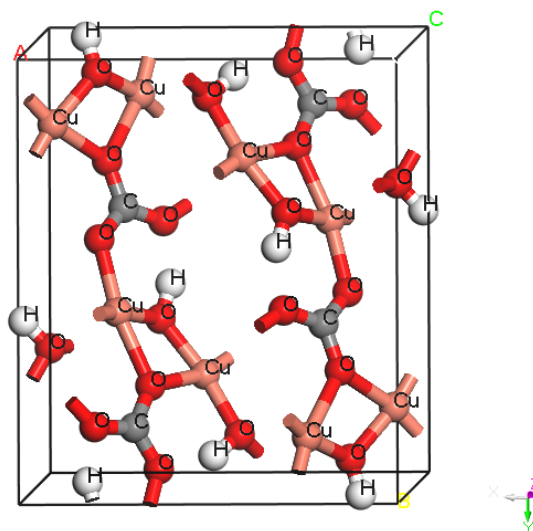


Fig. 10. Malachite crystal structure ($\text{C}_4\text{H}_8\text{O}_{20}\text{Cu}_8$)

Table 4. Mulliken population and the length of the bond in malachite

Bonds	Mulliken population	Length (Å)
C-O	0.90	1.30
H-O	0.59	1.03
Cu-O	0.22	2.01

The dissociation of minerals tends to the surface with the weakest atomic interaction, that is, the surface with the lowest energy (Wen et al., 2013). Integrated existing research data (Htay et al., 2014; Stenlid et al., 2016; Sun and Ceder, 2018), $(-2\ 0\ 1)$, $(0\ 1\ 0)$, and $(1\ 1\ 0)$ surfaces were calculated, the surface energy of malachite surfaces are shown in Table 5.

Table 5. Surface energy of malachite mineral surfaces/(kJ/mol)

Surfaces	(-2 0 1) surface	(0 1 0) surface	(1 1 0) surface
Surface energy	-34195.62	-34006.32	-34109.53

As shown in Table 5, (-2 0 1) surface in malachite with the lowest energy, which agreed with the previous work (Mao 2016; Wu et al., 2017), the (-2 0 1) surface was chosen as a surface model for adsorption calculations, the (-2 0 1) surface was cleaved from the optimized malachite crystal structure, based on the previous study (Mao, 2016; Wu et al., 2017), k-point sampling density of $2 \times 2 \times 1$ was used for all adsorption calculations, a vacuum thickness of 20 Å was placed between the slabs, and the (-2 0 1) surface configuration was optimized to conduct the reagents adsorption simulation. According to the study (Deng, 2015; Wu, 2017), the simulation was conducted in a vacuum, thus, the adsorption energy was calculated differently because the calculation systems vary, the results did not represent the actual energy but provided a qualitative basis. The research aimed to obtain change trend of the interaction energy between malachite surface and reagents, and explained experimental phenomena. Studying the adsorption energy of reagents on (-2 0 1) surface of malachite, the calculation results shown in Table 6 suggested that the addition of HS⁻ decreased the adsorption energy of C₄H₉OCSS⁻ on malachite (-2 0 1) surface, the changing trend of interaction energy was consistent with the previous report (Mao, 2016; Wu, 2017), the addition of Na₂S prior to NaBX improving the adsorption of NaBX on malachite surface, facilitating the flotation of malachite. Cu²⁺ increased the adsorption energy of HS⁻, decreased the sulfuration of the malachite surface. In addition, Cu²⁺ increased the adsorption energy of C₄H₉OCSS⁻ under sulfuration condition, reduced the adsorption of NaBX on malachite surface, depressed the sulfuration flotation of malachite.

Table 6. Adsorption energy of reagents on malachite (-2 0 1) surface /(kJ/mol)

Adsorption models	E _a	E _s	E _c	ΔE
Malachite + HS ⁻	-34938.92	-34195.62	-316.65	-426.65
Malachite + Cu ²⁺ + HS ⁻	-34897.75	-34195.62	-400.91	-301.22
Malachite + C ₄ H ₉ OCSS ⁻	-34843.12	-34195.62	-197.27	-450.23
Malachite + HS ⁻ + C ₄ H ₉ OCSS ⁻	-35702.81	-34195.62	-513.92	-993.27
Malachite + Cu ²⁺ + HS ⁻ + C ₄ H ₉ OCSS ⁻	-35375.50	-34195.62	-703.69	-476.19

Figure 11 shows the possible adsorption configuration of HS⁻ on malachite (-2 0 1) surface in the absence and presence Cu²⁺, and the values shown in the figure indicate the atomic distance in angstroms. As shown in Fig. 11(a), HS⁻ interacted with Cu on the (-2 0 1) surface of malachite mainly by S atom. The length and the Mulliken population of the Cu-S bond was 0.2382 nm, 0.23, separately. The length of the bond between the valence radius and the ionic radius, there was the chemical adsorption when HS⁻ on the malachite surface. As shown in Fig. 11(b), after the addition of Cu²⁺, the length and the Mulliken population of the Cu-S bond was 0.2213 nm, 0.30, separately, but the Cu were from pulp, not the malachite surface. The competitive adsorption for Na₂S between the Cu in pulp and Cu on the malachite surface depressed the sulfuration of malachite surface, inhibit the sulfuration flotation of malachite.

Figure 12 shows the possible adsorption configuration of C₄H₉OCSS⁻ on malachite (-2 0 1) surface under sulfuration condition in the absence and presence of Cu²⁺. As shown in Fig. 12(a), C₄H₉OCSS⁻ interacted with Cu²⁺ on the (-2 0 1) surface of malachite mainly by S atoms. For the S of single bond in C₄H₉OCSS⁻, the length and the Mulliken population of Cu-S bond were 0.218 nm, 0.33, separately. For the S of a double bond in C₄H₉OCSS⁻, the length and the Mulliken population of Cu-S bond were 0.229 nm, 0.30, separately. There was the chemical adsorption when C₄H₉OCSS⁻ on the malachite surface under sulfuration condition. After the addition of Cu²⁺, C₄H₉OCSS⁻ away from the malachite surface and close to the Cu²⁺ in the pulp. The competitive adsorption for NaBX between the Cu²⁺ in pulp and Cu²⁺ on the malachite surface depressed the sulfuration flotation of malachite. These results were consistent with the results of the flotation and adsorption experiments.

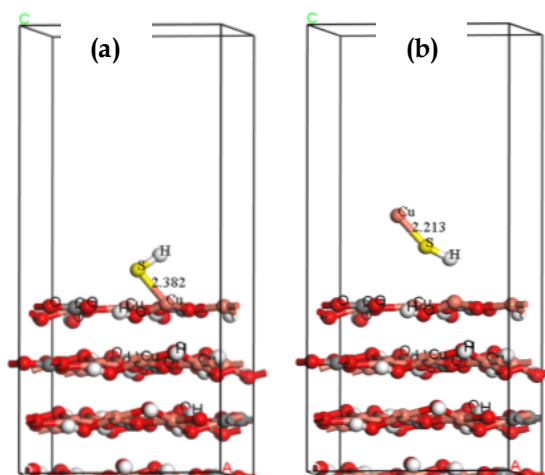


Fig. 11. Adsorption configuration of HS^- on malachite (-2 0 1) surface (a) in the absence (b) in the presence of Cu^{2+}

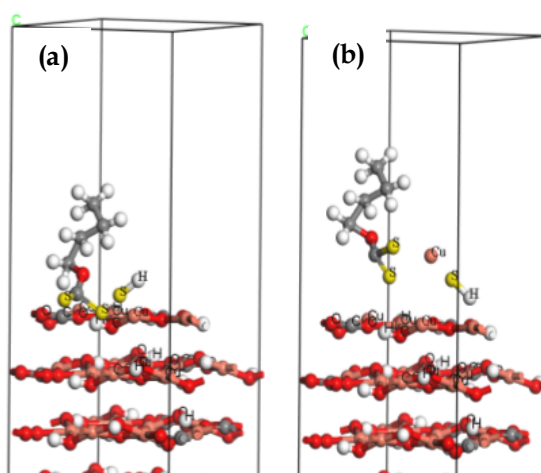


Fig. 12. Adsorption configuration of HS^- , $\text{C}_4\text{H}_9\text{OCSS}^-$ on malachite (-2 0 1) surface (a) in the absence (b) in the presence of Cu^{2+}

4. Conclusions

In this study, the effects of copper ions on the sulfidization flotation of malachite was studied, the results showed that the addition of Cu^{2+} ions depressed the malachite sulfidization flotation, the recovery of malachite decreased from 78.20% to 26.90% when the 150 mg/dm³ of CuSO_4 was added prior to Na_2S . The zeta-potential and the adsorption measurements, and XPS analysis indicated that the depression mechanism of Cu^{2+} ions included that the sulfidization of malachite was weakened, and the adsorption amount of collector on malachite surface decreased after the addition of Cu^{2+} ions. The calculation by Materials Studio revealed that adsorption energy of HS^- and $\text{C}_4\text{H}_9\text{OCSS}^-$ ions on the malachite surface increased after the adding of Cu^{2+} ions, competitive adsorption for HS^- and $\text{C}_4\text{H}_9\text{OCSS}^-$ made Cu^{2+} ions depress the sulfidization flotation of malachite. Overall, reducing the solubility of malachite mineral seems to be of great significance for improving its floatability, which will be beneficial for the adsorption of sulfidizing agents and collectors on malachite surface.

Acknowledgments

The authors gratefully acknowledge the financial support by General Program of National Natural Science Foundation of China (No. 51874072), the National Natural Science Foundation of China (No. 51504053), and the Fundamental Research Funds for the Central Universities (No. N170107013), the National Natural Science Foundation of China (No. 51804081), the Found of State Key Laboratory of Mineral Processing (No. BGRIMM-KJSKL-2017-14).

References

- BOULTON, A., FORNASIERO, D., RALSTON, J., 2003. *Characterisation of sphalerite and pyrite flotation samples by XPS and ToF-SIMS*. Int. J. Miner. Process. 70, 205-219.
- CASTRO, S., SOTO, H., GOLDFARB, J., LASKOWKI, J., 1974. *Sulphidizing reactions in the flotation of oxidized copper minerals, II. Role of the adsorption and oxidation of sodium sulphide in the flotation of chrysocolla and malachite*. Int. J. Miner. Process. 1(2), 151-161.
- CHEN, X., PENG, Y., BRADSHAW, D., 2014. *The separation of chalcopyrite and chalcocite from pyrite in cleaner flotation after regrinding*. Miner. Eng. 58, 64-72.
- CHOI, J., CHOI, S.Q., PARK, Y., HAN, Y., KIM, H., 2016. *Flotation behavior of malachite in mono- and di-valent salt solutions using sodium oleate as a collector*. Int. J. Miner. Process. 146, 38-45.
- CORIN, K.C., KALICHINI, M., O'CONNOR, C.T., SIMUKANGAB, S., 2017. *The recovery of oxide copper minerals from a complex copper ore by sulphidisation*. Miner. Eng. 102, 15-17.
- DENG, J.S., LEI, Y.H., WEN, S.M., CHEN, Z.X., 2015. *Modeling interactions between ethyl xanthate and Cu/Fe ions using DFT/B3LYP approach*. Int. J. Miner. Process. 140, 43-49.
- FENG, Q.C., WEN, S.M., ZHAO, W.J., DENG, J.S., XIAN, Y.J., 2015. *Adsorption of sulfide ions on cerussite surfaces and implications for flotation*. Appl. Surf. Sci. 360, 365-372.
- FENG, Q.C., WEN, S.M., DENG, J.S., ZHAO, W.J., 2017. *Combined DFT and XPS investigation of enhanced adsorption of sulfide species onto cerussite by surface modification with chloride*. Appl. Surf. Sci. 425, 8-15.
- FENG, Q.C., ZHAO, W.J., WEN, S.M., CAO, Q.B., 2017. *Copper sulfide species formed on malachite surfaces in relation to flotation*. J. Ind. Eng. Chem. 48, 125-132.
- FENG, Q.M., ZHAO, W.J., WEN, S.M., 2018. *Surface modification of malachite with ethanediamine and its effect on sulfidization flotation*. Appl. Surf. Sci. 436, 823-831.
- FENG, Q.C., ZHAO, W.J., WEN, S.M., 2018. *Ammonia modification for enhancing adsorption of sulfide species onto malachite surfaces and implications for flotation*. J. Alloys. Compd. 744, 301-309.
- HARVEY, D.T., LINTON, R.W., 1984. *X-ray photoelectron spectroscopy (XPS) of adsorbed zinc on amorphous hydrous ferric oxide*. Colloids Surf. 11, 81-96.
- HOPE, G.A., WOODS, R., PARKER, G.K., BUCKLEY, A.N., MCLEAN, J., 2010. *A vibrational spectroscopy and XPS investigation of the interaction of hydroxamate reagents on copper oxide minerals*. Miner. Eng. 23, 952-959.
- HTAY, M.T., OKAMURA, M., YOSHIZAWA, R., HASHIMOTO, Y., ITO, K., 2014. *Synthesis of a cuprite thin film by oxidation of a Cu metal precursor utilizing ultrasonically generated water vapor*. Thin Solid Films. 556, 211-215.
- HUANG, Y.G., LIU, G.Y., LIU, J., YANG, X.L., ZHAN, Z.Y., 2018. *Thiadiazole-thione surfactants: Preparation, flotation performance and adsorption mechanism to malachite*. J. Ind. Eng. Chem. 67, 99-108.
- HUANG, K.H., CAO, Z.F., WANG, S., YANG, J., HONG, Z. H., 2019. *Flotation performance and adsorption mechanism of styryl phosphonate mono-iso-octyl ester to malachite*. Colloids Surf., A. 579, 8.
- KHMELEVA, T.N., SKINNER, W., BEATTIE, D.A., 2005. *Depressing mechanisms of sodium bisulphite in the collectorless flotation of copper-activated sphalerite*. Int. J. Miner. Process. 76, 43-53.
- LI, F., ZHONG, H., XU, H., JIA, H., LIU, G., 2015. *Flotation behavior and adsorption mechanism of γ -hydroxyoctyl phosphinic acid to malachite*. Miner. Eng. 71, 188-193.
- LI, Y.Q., CHEN, J.H., KANG, D., GUO, J., 2012. *Depression of pyrite in alkaline medium and its subsequent activation by copper*. Miner. Eng. 26, 64-69.
- LIU, G.Y., HUANG, Y.G., QU, X.Y., XIAO, J.J., YANG, X.L., XU, Z.H., 2016. *Understanding the hydrophobic mechanism of 3-hexyl-4-amino-1, 2,4-triazole-5-thione to malachite by ToF-SIMS, XPS, FTIR, contact angle, zeta potential and micro-flotation*. Colloids Surf., A. 503, 34-42.
- LIU, C., ZHU, G.L., SONG, S.X., LI H.Q., 2018. *Interaction of gangue minerals with malachite and implications for the sulfidization flotation of malachite*. Colloids Surf., A. 555, 679-684.
- LIU, S., ZHONG, H., LIU, G.Y., XU, Z.H., 2018. *Cu(I)/Cu(II) mixed-valence surface complexes of S-(2-hydroxyamino)-2-oxoethyl -N,N-dibutylthiocarbamate: Hydrophobic mechanism to malachite flotation*. J. Colloid Interface Sci. 512, 701-712.
- LOTTER, N.O., BRADSHAW, D.J., BARNES, A.R., 2016. *Classification of the Major Copper Sulphides into semiconductor types, and associated flotation characteristics*. Miner. Eng. 96-97, 177-184.
- MAO, Y.B., 2016. *Flotation theoretical and experimental study on reinforced sulfuration flotation of malachite by ammonium-ammine salt*. Kunming: Kunming University of Science and Technology, 1-6.

- MULLIKEN, R.S., 2004. *Electronic Population Analysis on LCAO–MO Molecular Wave Functions*. I. J. Chem. Phys. 23, 1833.
- PARK, K., PARK, S., CHOI, J., KIM, G., TONG, M., KIM, H., 2016. *Influence of excess sulfide ions on the malachite-bubble interaction in the presence of thiol-collector*. Sep. Purif. Technol. 168, 1-7.
- POWELL, K.J., BROWN, P.L., BYRNE, R.H., GAJDA, T., HEFTER, G., SJOBERG, S., WANNER, H., 2007. *Chemical speciation of environmentally significant metals with inorganic ligands Part 2: The Cu^{2+} -OH⁻, Cl⁻, CO_3^{2-} , SO_4^{2-} and PO_4^{3-} systems (IUPAC Technical Report)*. Pure Appl. Chem. 79, 895-950.
- SHEN, P.L., LIU, D.W., ZHANG, X.L., JIA, X.D., SONG, K.W., LIU, D., 2019. *Effect of $(\text{NH}_4)_2\text{SO}_4$ on eliminating the depression of excess sulfide ions in the sulfidization flotation of malachite*. Miner. Eng. 137, 43-52.
- SRDJAN, M.B., 2010. *Handbook of Flotation Reagents: Chemistry, Theory and Practice: Volume 2. Flotation of Gold, PGM and Oxide Minerals*. Amsterdam: Elsevier Science. 47–50.
- STENLID, J.H., SOLDEMO, M., JOHANSSON, A J., LEYGRAF, C., GOTHELID, M., WEISSENRIEDER, J., BRINCK, T., 2016. *Reactivity at the $\text{Cu}_2\text{O}(100)$: Cu - H_2O interface: a combined DFT and PES study*. Phys. Chem. Chem. Phys. 18, 30570-30584.
- SUN, W., SU, J.F., ZHANG, G., HU, Y.H., 2012. *Separation of sulfide lead-zinc-silver ore under low alkalinity condition*. Journal of Central South University. 19, 2307-2315.
- SUN, W., CEDER, G., 2018. *A topological screening heuristic for low-energy, high-index surfaces*. Surf. Sci. 669, 50-56.
- SUSSE, P., 1966. *Verfeinerung der Kristallstruktur des Malachits, $\text{Cu}_2(\text{OH})_2\text{CO}_3$* . Acta Crystallogr. 53, 80.
- WEN, S.M., DENG, J.S., XIAN, Y.J., XIAN, Y.J., LIU, D., 2013. *Theory analysis and vestigial information of surface relaxation of natural chalcopyrite mineral crystal*. T. Nonferr. Metal. Soc. 23, 796-803.
- WU, D.D., MA, W.H., MAO, Y.B., DENG, J.S., WEN, S.M., 2017. *Enhanced sulfidation xanthate flotation of malachite using ammonium ions as activator*. Sci. Rep. 7, 2086.
- WU, D.D., MAO, Y.B., DENG, J.S., WEN, S.M., 2017. *Activation mechanism of ammonium ions on sulfidation of malachite (-201) surface by DFT study*. Appl. Surf. Sci. 410, 126-133.
- YIN, W.Z., SUN, Q.Y., LI, D., TANG, Y., FU, Y.F., YAO, J., 2019. *Mechanism and application on sulphidizing flotation of copper oxide with combined collectors*. T. Nonferr. Metal. Soc. 29, 178–185.
- ZHOU, L.G., 2007. *Ore Mineralogy Bases, The Third Edition [M]*. Beijing: Metallurgical Industry Press, 20–91.